Advances in Concrete Construction, *Vol. 5, No. 5 (2017) 451-468*
DOI: https://doi.org/10.12989/acc.2017.5.5.451

Behavior of one way reinforced concrete slabs with styropor blocks

Adel A. Al-Azzawi*, Abbas J and Al-Asdi[a]

Department of Civil Engineering, Al-Nahrain University, Baghdad, Iraq

(Received Ocotber 28, 2016, Revised August 26, 2017, Accepted September 4, 2017)

Abstract. The problem of reducing the self-weight of reinforced concrete structures is very important issue. There are two approaches which may be used to reduced member weight. The first is tackled through reducing the cross sectional area by using voids and the second through using light weight materials. Reducing the weight of slabs is very important as it constitutes the effective portion of dead loads in the structural building. Eleven slab specimens was casted in this research. The slabs are made one way though using two simple supports. The tested specimens comprised three reference solid slabs and eight styropor block slabs having (23% and 29%) reduction in weight. The voids in slabs were made using styropor at the ineffective concrete zones in resisting the tensile stresses. All slab specimens have the dimensions (1100× 600×120 mm) except one solid specimens has depth 85 mm (to give reduction in weight of 29% which is equal to the styropor block slab reduction). Two loading positions or cases (A and B) (as two-line monotonic loads) with shear span to effective depth ratio of (a/d=3, 2) respectively, were used to trace the structural behavior of styropor block slab. The best results are obtained for styropor block slab strengthened by minimum shear reinforcement with weight reduction of (29%). The increase in the strength capacity was (8.6% and 5.7%) compared to the solid slabs under loading cases A and B respectively. Despite the appearance of cracks in styropor block slab with loads lesser than those in the solid slab, the development and width of cracks in styropor block slab is significantly restricted as a result of presence a mesh of reinforcement in upper concrete portion.

Keywords: monotonic load; one-way slab; structural behavior; styropor block; weight reduction

1. Introduction

Reinforced concrete slabs together with other supporting structural elements or members such as beams, drops and ribs are called structural floor system. It is often in direct contact with gravity load and transferring it to the rest of vertical elements such as columns, walls and then to foundations. The self-weight of slab comprises the largest proportion of the superstructure weight of multistory buildings. For this reason, the reduction of slab weight is very effective issue, especially with long spans members and multistory buildings that in turn reduce the cross sectional areas of all building structural members and therefore reducing the load transmitted to soil.

*Corresponding author, Assistant Professor, E-mail: dr_adel_azzawi@yahoo.com
[a]MSc. Student, E-mail: abbas19asdi@yahoo.com

http://www.techno-press.org/?journal=acc&subpage=7 ISSN: 2287-5301 (Print), 2287-531X (Online)

Reinforced concrete hollow block slab is designed to reduce the dead load of slab and to simplify formwork. It is an important type of voided slab and commonly used in long span floor system. The hollow blocks are used to occupy portions of the slab thickness and this will leads to give deeper lever arm for the rebar and saving concrete material and hence decreasing slab self-weight. The reinforcement bars are placed in the slab ribs between the blocks. The used blocks in slabs may be styro-foam or hollow concrete blocks.

Many researches around the world focus on studying concrete slab such as Gorkem and Husem (2013) and Yu *et al*. (2016) and others on reducing slab weight by removing area from the ineffective zone along cross section of the slab. Abdul-Wahab and Khalil (2000) carried an experimental tests on eight (1/4) scale waffle slab models with different or varied rib spacing and rib depth. Lau and Clark (2011) carried out experimental tests on three series (consisting of twenty-six samples) to determine the efficiency of the wide beams to shear failure. The first with an internal column and four equal point loads were distributed on four beams with equal distances. The second case was similar to the first case but with different loads and the third case with an edge column. Olawale and Ayodele (2014) tested waffle and solid slab specimens. Allawi (2014) carried out experimental tests on one-way voided slab to investigate the structural behavior of the reinforced concrete slabs containing cavities. de Oliveira *et al*. (2014) carried out experimental investigation on eight one way ribbed slab specimens in order to detect the contribution of slab portion in resisting the applied shear. Al-Azzawi and Abed (2017) investigated experimentally the behavior of reinforced concrete slabs with hollow cores under varying study parameters. The experimental part included testing 8 slab specimens of solid and hollow-core models with (2.05 m) length, (0.6 m) width and (25 cm) thickness under two monotonic line loads. All the previous researches showed encouraging results which leads to the development of economical and effective systems in terms of structural behavior compared to solid slab traditional floor systems. Through previous studies, hollow blocks were used in thin slabs while in the present research it is made in moderately thick slabs and their shear and flexural behavior are investigated in details. In general, the challenge in using hollow block slabs was preventing the shear failure of these slabs which may happen due to making the voids in slabs. Many previous researches were carried out to study the shear behavior of these thin slabs, numerically and analytically but few of them carried experimental investigation for studying the behavior of thick slabs. In this study, the structural behavior of one way reinforced concrete thick slabs with and without blocks was adopted experimentally.

2. Experimental work

2.1 Study parameters

The eleven tested specimens in this research are classified according to Fig. 1. The weight reduction effect on structural behavior is represented by the percentage of styropor used in the slab cross section. The response of styropor block slab under monotonic loading is studied through different line load positions (A and B) (i.e., shear span to effective depth (a/d)) and the effect of the ribs arrangement or distribution on the styropor block structural floor system. The effect of increasing of the styropor block slab stiffness through increasing the depth of ribs and the effect of increasing the shear capacity using shear reinforcement or concrete tapered width section at critical shear zone are also investigated.

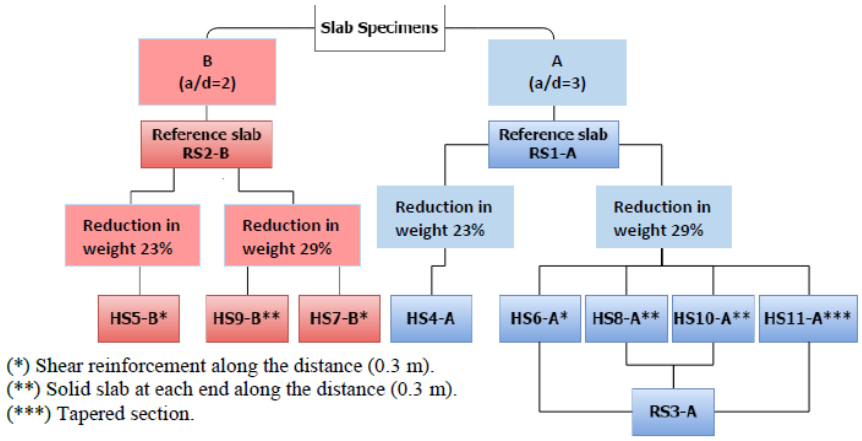

Fig. 1 Arrangement of parameters

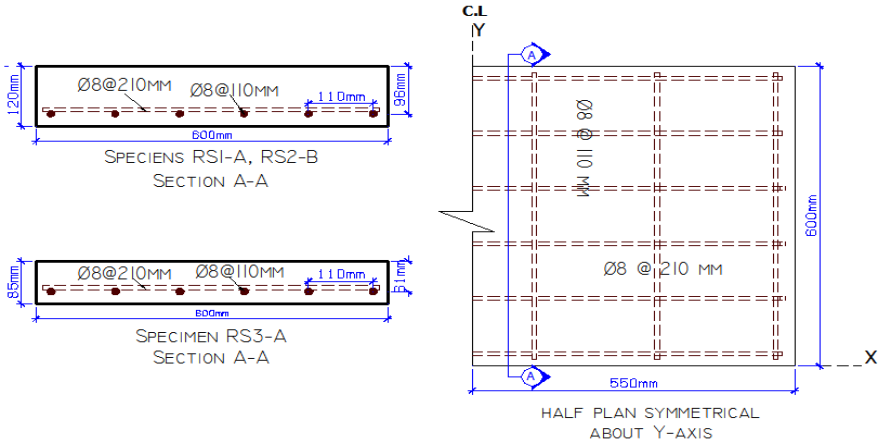

Fig. 2 Reinforcement details of specimens RS1-A, RS2-Band RS3-A

2.2 Slab specimens details

Eleven slab specimens have been casted for this study. All the casted slab specimens have the dimensions (1100×600×120 mm) except one specimen (RS3-A) has same length and width but different depth of (85 mm). Longitudinal or flexural reinforcement of (6Ø8 mm) for each slab specimen was used.

Three solid slab specimens (RS1-A, RS2-B and RS3-A) were the reference slabs (RS), which were provided by transverse reinforcement (Ø8@210 mm) in the unsupported direction. The details of reinforcement for specimens (RS1-A, RS2-B and RS3-A) are shown in Fig. 2.

Eight slab specimens have casted as styropor block slabs (HS). The thickness of slab portion is equal to 50 mm which was reinforced by mesh (Ø4@110 mm) in each direction and located at the center of slab portion. They can be classified or described as follows:

• HS4-A and HS5-B slab specimens have self-weight reduction equal to 23%. Both specimens consist of three ribs (rib depth×rib width b_w) (120×120 mm) with longitudinal reinforcement (2Ø8

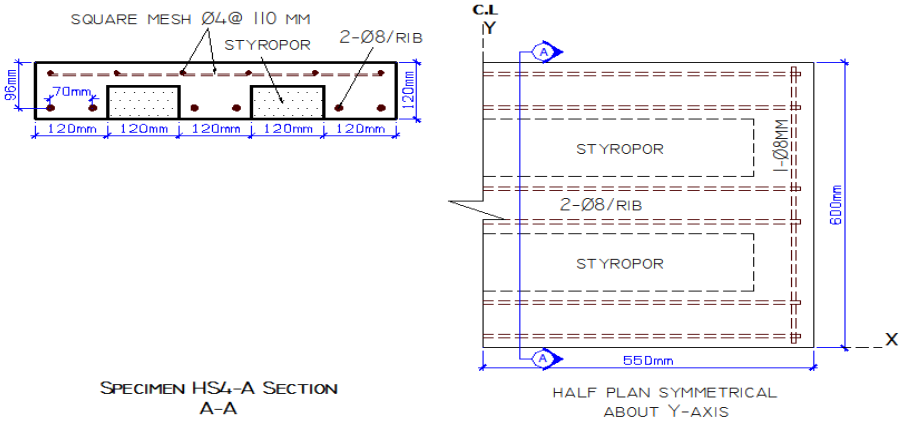

Fig. 3 Reinforcement details of specimen HS4-A

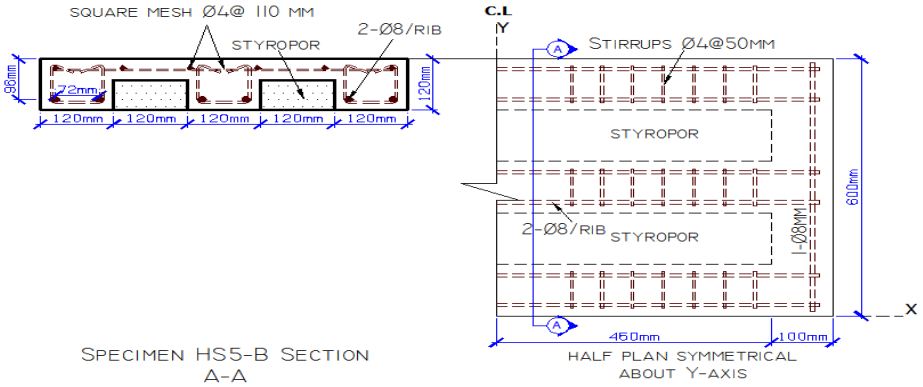

Fig. 4 Reinforcement details of specimen HS5-B

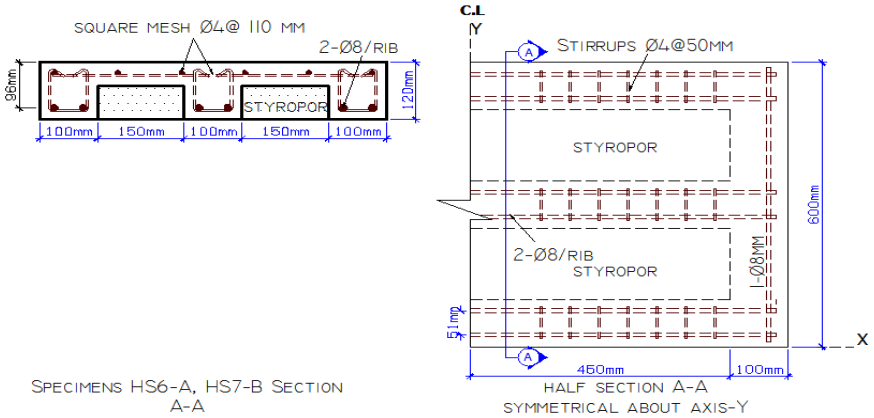

Fig. 5 Reinforcement details of specimens HS6-A and HS7-B

mm/rib). HS5-B specimen was strengthened by minimum shear reinforcement (Ø4@ 50 mm) at the critical shear region. Figs. 3 and 4 illustrate the reinforcement details for specimens HS4-A and HS5-B respectively.

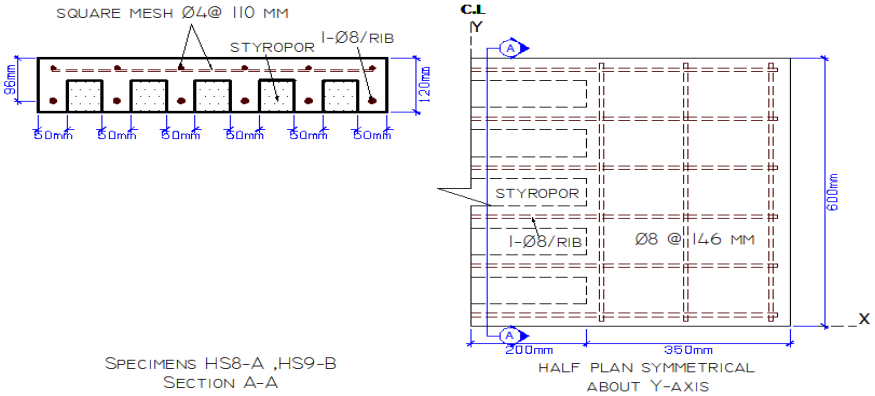

Fig. 6 Reinforcement details of specimens HS8-A and HS9-B

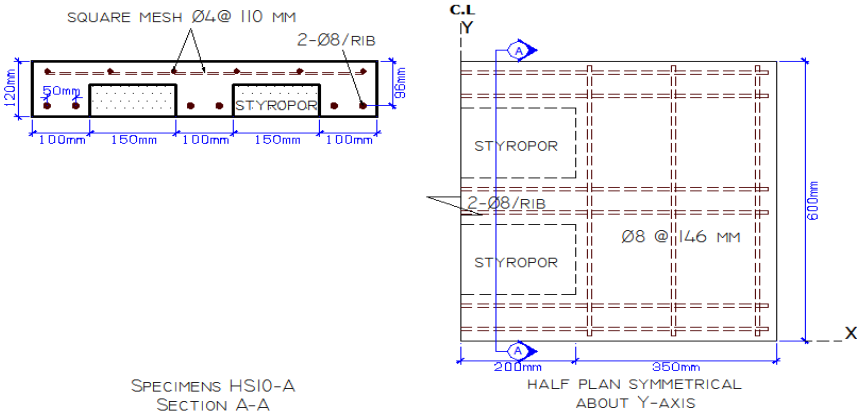

Fig. 7 Reinforcement details of specimen HS10-A

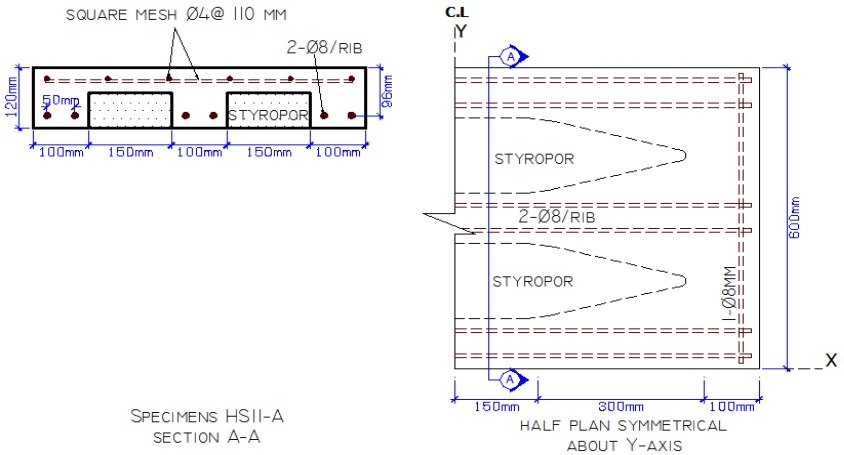

Fig. 8 Reinforcement details of specimen HS11-A

• HS6-A and HS7-B slab specimens consist of three ribs (120×100 mm) with longitudinal reinforcement (2Ø8 mm/rib), they were strengthened by minimum shear reinforcement (Ø4@50

Table 1 Concrete mix proportions

Cement content (kg/m^3)	Sand (kg/m^3) with Max. size 4.75 mm	Gravel (kg/m^3) with Max. size 10 mm	Superplastsizer by weight of cement	Water/cement	Slump (mm)
370	750	1050	0.7	0.38	80-100

Table 2 Hardened concrete characteristics

Specimen	Compressive strength (f'_c) (MPa)	Splitting tensile strength (f_{ct}) (MPa)	Modulus of rupture (f_r) (MPa)	Modulus of Elasticity (E_C) (MPa)
RS1-A, RS2-B	37.31	3.49	3.84	32152
RS3-A, HS4-A, HS5-B	37.96	3.61	4.2	30404
HS6-A, HS7-B	36.76	3.72	3.9	30490
HS8-A, HS9-B	37.7	3.55	4.1	33475
HS10-A, HS11-B	38.26	3.91	3.88	29652

mm) at the critical shear zone as shown in Fig. 5. Both specimens have self-weight reduction equal to 29%.

• HS8-A and HS9-B slab specimens are casted with a solid slab portion for length of (300 mm) at each end of the specimens and six ribs (h=120 mm×b_w=50 mm) with longitudinal reinforcement (1Ø8 mm/rib) as shown in Fig. 6. Both specimens have self-weight reduction equal to 29%.

• HS10-A specimen is similar to HS8-A specimen except that the size of ribs is different which consist of three ribs (120×100 mm) having longitudinal reinforcement of (2Ø8 mm/rib) as shown in Fig. 7.

• HS11-A specimen has weight reduction equal to 29% and is provided by tapered concrete styropor shape at critical shear region as shown in Fig. 8.

The design calculations for all slab specimens are based on ACI-318 (2014) and considering all limitations mentioned in the code.

2.3 Material

Concrete mix quantities for all casted slab specimens are given in the Table 1. The properties of hardened concrete (compressive strength, splitting tensile strength and modulus of elasticity) are obtained by testing cylindrical specimens (150×300 mm). The modulus of rapture is obtained by testing prism specimens (100×100×300 mm) and computed as average of three control specimens for each group as listed in the Table 2.

2.4 Specimens loading test

All slabs specimens were prepared and tested as one-way slab (supported on two opposite sides) using a 1000 kN hydraulic testing machine under monotonic load up to failure, at the laboratory of Civil Engineering Department/Al-Nahrain University. The tests of slabs were carried out at age of 30-40 days. The positions of supports were indicated on sides of specimens according to effective span. The loads were applied at increments rate of 1 kN/sec. At each increment of monotonic load, all measurements from the dial gauge at mid span and automatically at the

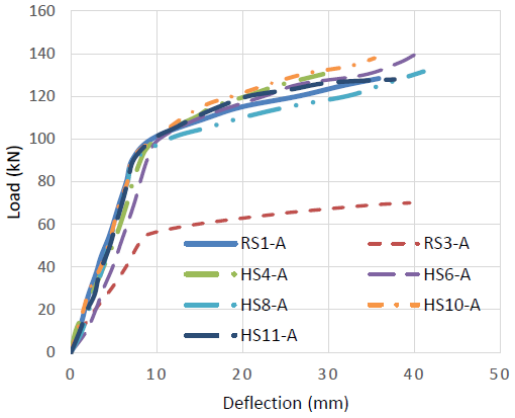

Fig. 9 Load mid span deflection curves for load case or position (A)

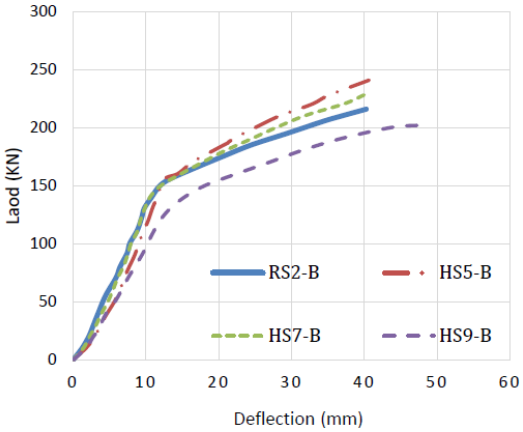

Fig. 10 Load mid span deflection curves for load case or position (B)

position of applied load were made. First moment crack loads (P_{cr}) and corresponding displacement (Δ_{cr}) were marked, the developing cracks were traced, and then the ultimate loads-deflection were recorded.

2.5 Experimental results of slab specimens

The test results of eleven slab specimens can be classified in two groups (A) and (B) according to the position of line loads or shear span to effective depth (a/d ratio). The results of group (A) include testing seven slab specimens under two line loads of (a/d=3) while the results of group (B) include testing four slab specimens with (a/d=2). The relationship between the applied loads versus mid-span deflection during testing is illustrated in Figs. 9 and 10 and the results of cracking and ultimate load-mid span deflection which have obtained from experimental work and the relation-ship between cracking and ultimate stages for eleven slab specimens are listed in Table 3.

It can be observed from the load-displacement relationship that all specimens fail after yielding of tensile reinforcement with considerable deformation. The first reason refers to the provided longitudinal reinforcement ratio (ρ) in the reference slabs and the styropor block slab (which was

Table 3 Experimental results

Specimens	a/d	Cracking load (P_{cr}) (KN)	Mid-span deflection(Δ_{cr}) at (P_{cr}) (mm)	Ultimate load (P_u) (KN)	Mid-span deflection (Δu) at (P_u) (mm)	$(\frac{P_{cr}}{P_u})$ %	$(\frac{\Delta_{cr}}{\Delta_u})$ %
RS1-A	3	37.2	2.48	128.37	35.8	29%	7%
RS2-B	2	55.20	3.06	215.80*	40.2	26%	8%
RS3-A	3	20.00	2.56	70.07	39.8	29%	6%
HS4-A	3	30.63	2.55	130.43**	29.5	23%	9%
HS5-B	2	38.43	3.11	240.76	40.6	16%	8%
HS6-A	3	28.00	3.26	139.37	40.0	20%	8%
HS7-B	2	38.70	2.61	228.00	40.0	17%	7%
HS8-A	3	23.43	2.14	131.63	41.1	18%	5%
HS9-B	2	25.50	2.40	202.06*	48.0	13%	5%
HS10-A	3	28.77	1.87	137.90	35.4	21%	5%
HS11-A	3	27.13	2.50	127.93	37.6	21%	7%

(*) Diagonal shear failure. (**) Combined flexural-shear failure. Ductile flexural failure for remaining slabs

Table 4 Comparison between experimental and ACI 318 ultimate load

Specimens	a/d	Experimental ultimate load (P_u)	Theoretical ultimate load (P_n)	Experimental load/theoretical load
RS1-A	3	128.37	100.67	1.28
RS2-B	2	215.80	119.2*	1.81
RS3-A	3	70.07	62.50	1.12
HS4-A	3	130.43	79.63*	1.69
HS5-B	2	240.76	151.00	1.63
HS6-A	3	139.37	100.67	1.39
HS7-B	2	228	151.00	1.51
HS8-A	3	131.63	100.67	1.31
HS9-B	2	202.06	120.20*	1.68
HS10-A	3	137.90	100.67	1.37
HS11-A	3	127.93	100.67	1.27

(*****)P_n: Controlled by theoretical shear capacity

designed assuming T section according to ACI- 318 (2014) is lesser than the maximum steel ratio (ρ_{max}).The second reason is attributed to the concrete cross-section which has a sufficient shear strength (V_n) even without shear reinforcement which permit the occurrence of a considerable vertical deformation (due to normal stress) before the failure.

From Table 3, the solid slabs (RS) exhibit the highest percentage of cracking load to ultimate load (26% to 29%) and this is due to the contribution of concrete with large cross sectional area under neutral axis to resist the tensile stresses. For styropor block slabs (HS), the decreasing for this ratio refers to two reasons. The first reason is the decreasing in the cross sectional area under neutral axis and the second refers to the increase in the ultimate load capacity of styropor block

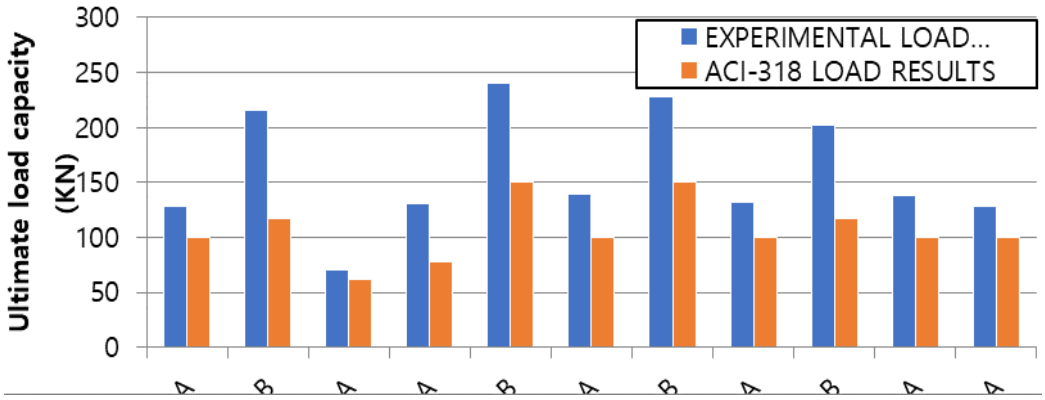

Fig. 11 Comparison between experimental and theoretical ultimate load

slabs compared to the solid slab. It can be noted that there is no effect for the longitudinal reinforcement in pre-cracking stage. For example, under the same percentage of (P_{cr}/P_u) the reinforcement ratios (ρ) of slabs RS1-A and RS3-A are 0.0052 and 0.0082 respectively. On other hand, the increase in the ultimate load capacity of styropor block slabs are associated by improving the shear capacity using shear reinforcement or solid slab at critical shear region and the characteristics of concrete at compression zone using upper mesh reinforcement which have significant effect on the percentage of (P_{cr}/P_u) .

The percentages of the mid-span deflection at cracking to the ultimate stages are ranging (5% to 9%) for all slab specimens. It is influenced by magnitude of reduction in cross sectional area and significantly by the elastic and plastic deformations provided by longitudinal reinforcement.

2.5.1 Comparison between experimental results and the predicted results by ACI 318

The comparison between the experimental results and the results computed according to the ACI-318 (2014) equations for ultimate loads are shown in the Table 4 and Fig. 11. This comparison is very important to provide the designer with detailed information about the conservations taken out by ACI 318 equation used in the design of slabs.

For specimens that fail in flexure mode, there is a difference between the results obtained from the experimental work ultimate load (P_u) and those computed according to the ACI-318 (2014) nominal load (P_n) equations. This is may be due to that the ultimate strength method which is adopted by ACI 318 assumed uniaxial state of stresses in one-way slab and neglected the effect of Poisson's ratio. This code assumption is almost accurate for the case of beams, but in case of slab (has smaller depth but greater width) the situation is rather different. The slab can resist more loads than that computed by the ACI-318 equations and this is due to the small transverse stresses developed in slab width direction.

With regard to the specimens (RS2-B, HS4-A and HS9-B) which (P_n) controlled by theoretical shear capacity, one of the reasons for the obvious difference in results refers to that ACI 318 code computed the shear strength capacity (V_C) according to

$$V_c = 0.17 \sqrt{f_c'}\ b.d \tag{1}$$

where *b* is the slab width and *d* is the effective slab depth. This equation neglects the effect of longitudinal reinforcement. The validity for shear strength equation mentioned in the code is

Table 5 Comparison of cracking load capacity between RS and HS under load case or position (A)

Specimens	a/d	R_w %	P_{cr} (KN)	R_{cr}
RS1-A	3	-	37.27	1.00
RS3-A		29	20.00	0.54
HS4-A		23	30.63	0.82
HS6-A		29	28.00	0.75
HS8-A		29	23.43	0.63
HS10-A		29	28.77	0.77
HS11-A		29	27.13	0.73

Table 6 Comparison of cracking load capacity between RS and HS under load case or position (B)

Specimens	a/d	R_w %	P_{cr} (KN)	R_{cr}
RS2-B	2	-	55.20	1.00
HS5-B		23	38.43	0.70
HS7-B		29	38.70	0.70
HS9-B		29	32.70	0.59

limited to beams or one-way solid slabs. The shear strength capacity for styropor block slab is computed according to ACI- 318 (2014) as follows

$$V_c = 1.1 * 0.17\sqrt{f_{c'}}\ b_w.d \quad (2)$$

The shear capacity of slabs depends on the ribs cross section and eliminates the contribution of bottom longitudinal rib reinforcement, top mesh reinforcement and the size of flange in calculating shear strength capacity. It can be concluded that the ACI 318 equations are very conservative to shear failure compared with EN-1991 (EC-2:2004), code which take into account the effect of increasing the member depth (size effect) and the ratio of longitudinal reinforcement into consideration. Birgison, (2011) obtained results of (P_u/P_n) between (1.47- 2.2) controlled by shear failure of six beams with different (a/d) ratio and depth, ACI 318 procedure was adopting in Birgison's study. The shear strength (V_C) of slabs is increased with increasing the flange thickness as stated in the research of de Oliveira, *et al*. (2014). They showed that 40% is the percentage increase in shear capacity of one way-ribbed slab specimens with overall depth of (300 mm) for flange thickness magnitude increased from (30 to 100 mm).

2.5.2 Effect of void dimensions on cracking load capacity

Generally, the reduction in cross section area of slabs or beams will cause a reduction in its cracking load capacity. This reduction may be due to the decrease in the slab 2nd moment of area caused by concrete removal between ribs. Tables 5 and 6 show the results of the cracking load capacity for A and B loading cases or positions. The symbol (R_{cr}) represents the ratio of cracking load capacity of slab specimen to cracking load capacity of reference solid slab specimen with overall depth of (120 mm).

The results indicate that the appearance of first cracks depends on void dimensions, magnitude of reduction in cross-sectional area of slab specimens and shear span to effective depth ratio. The second moment of area is a function of the slab cross section shape and the magnitude of the

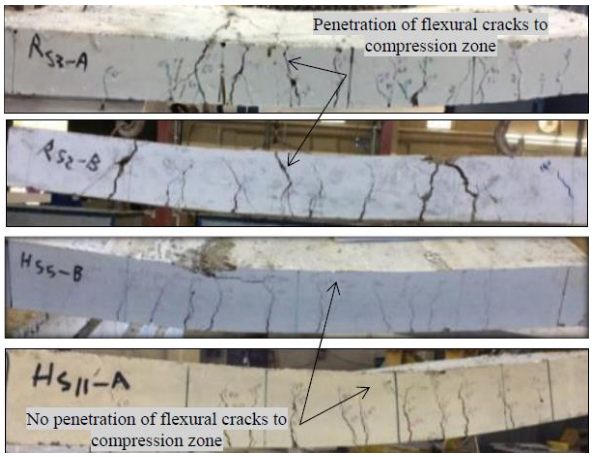

Fig. 12 Development of cracks in both solid and styropor block slab

reduction in cross sectional area. From Table 5, RS3-A solid slab with a reduction in cross sectional area of (29%) has the lowest value of cracking load capacity compared to all specimens. The solid slab specimens RS1-A has the highest value of cracking load for (a/d=3). The styropor block specimens with the same rib dimensions (120 mm depth×100 mm width) HS6-A, HS10-A and HS11-A have cracking load capacity higher than that obtained for the solid slab RS3-A with thickness of (85 mm). The four slabs have the same reduction in weight percentage and (a/d) ratio with different moment of inertia. The second moment of area of styropor block slabs is higher than that in the solid slab under the same cross-sectional area.

The comparison between HS8-A and HS10-A specimens which have the same characteristics of cross section (cross sectional area and 2nd moment of area), with different rib width of 50 mm and 100 mm respectively is made. The results show that the cracking load capacity of specimen HS10-A is higher than that in specimen HS8-A. The main reason is probably that the distribution of loads along the width of slab specimen is not regular. This will generate the concentration of normal stresses in the tensile zone on specific ribs. Nevertheless, this case is a good practical example, where it is difficult to distribute loads along the width of large space.

Another comparison is made between results for specimens which have shear span to effective depth of (a/d=3) and (a/d=2). It is well known that whenever the value of shear span (a) is increased, the applied load that generates a normal tensile stress equal to tensile strength of concrete is decreased. This is evident by reviewing the results of both positions of (a/d). This means that the cracking load increased with decreasing (a/d).

Small effect is noted at this stage of loading regarding the condition of shear span zone on the magnitude of cracking load capacity such as the existence of shear reinforcement, solid slab portion and tapered concrete section. For example, the values of cracking load capacity for slab specimens HS6-A, HS10-A and HS11-A with weight reduction 29% are (28, 28.77and 27.13 kN) respectively. It can be said that cracks occur at the critical flexural section whenever the normal tensile stress exceeds the tensile strength of concrete.

Despite the appearance of cracks in styropor block slab with loads lesser than those in the solid slab, the development and width of cracks in styropor block slab is significantly restricted as a result of presence a mesh of reinforcement in upper concrete portion. Photographic presentations are shown in Fig. 12 for final stages of cracks in both solid and styropor block slabs.

Table 7 Comparison of ultimate load capacity between RS and HS under loading case or position(A)

Specimens	a/d	R_w %	Ultimate load capacity P_u (KN)	Ultimate deflection Δ_u (mm)	R_u
RS1-A (reference)		-	128.37	35.8	1.000
RS3-A		29.	70.07	39.5	0.546
HS4-A		23	130.43	29.37	1.016
HS6-A	3	29	139.37	40.0	1.086
HS8-A		29	131.63	41.1	1.025
HS10-A		29	137.90	35.387	1.074
HS11-A		29	127.93	37.7	1

Table 8 Comparison of ultimate load capacity between RS and HS under loading case (B)

Specimens	a/d	R_w %	Ultimate load capacity P_u (KN)	Ultimate deflection Δ_u (mm)	R_u
RS2-B (reference)		-	215.80	40.2	1.000
HS5-B	2	23	240.76	40.6	1.116
HS7-B		29	227.90	40.0	1.057
H9-B		29	202.06	48.0	0.936

2.5.3 Effect of void dimensions on ultimate load capacity

Ultimate load- mid span deflections for slabs under two loading cases or positions (A) and (B) are listed in Tables 7 and 8. The ultimate load parameter with symbol (R_u) is used for comparison. The parameter represents the ratio of the ultimate load capacity of the slab under consideration to that of the reference solid slab with overall depth of (120) mm.

For the loading case (A), the R_u parameter or indicator of slab ultimate load capacity which have obtained from experimental work was found to be in the range of (1 to 1.086) compared to the reference slab as given in Table 7. HS4-A slab with reduction weight of 23% has an increase percentage in the load capacity of 1.6% compared to the RS1-A while this percentage reaches about 8.6% for the HS6-A slab. It can be observed that using shear reinforcement at critical shear zone in HS6-A slab increased the shear resistance of slab (V_n) in spite that the weight reduction in HS6-A slab is more than that in HS4-A slab. The HS4-A and HS6-A slabs are provided by reinforcement mesh at the top flange which restricts the crushing of concrete at compression zone compared to the reference slab RS1-A in which crushing occurred eventually in higher loads.

The results of slab specimens HS8-A and HS10-A which has the same cross sectional area and 2^{nd} moment of area, show that R_u parameter is increased compared to the reference slab by about (2.5 to 7.4%). Existence of solid slab portion on both ends of slab and enhancing the flange by reinforcement mesh lead to increase the ultimate load capacity. The solid slab portion contributes in increasing the flexural rigidity and the resistance to shear stresses, similar to that in wide beams. The results of deflection and load capacity for slab specimen HS11-A (R_w=29%) are almost equal to that in RS1-A specimen. HS11-A slab is provided by a variable cross-section along the shear span which increases the shear capacity. Also, the slab flange is provided by reinforcement mesh at the compression zone. At the same weight reduction (R_w=29%) the results of solid slab RS3-A show a decreasing in ultimate load by 45.4% compared to RS1-A and accompanied with increasing the value of deflection. The significant variation in results refers to the reduction in the

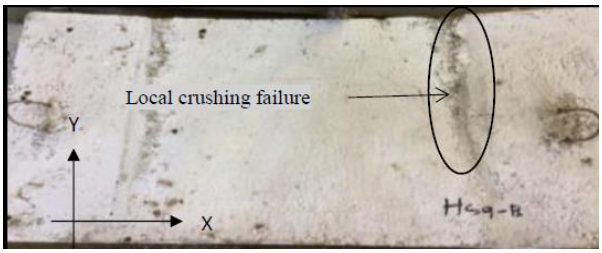

Fig. 13 Local crushing failure on the upper face of specimen HS9-B

Table 9 Failure mode for specimens tested under loading case (A)

Specimens	a/d	Ultimate load P_u (KN)	Displacement Δ_u at P_u (mm)	Mode of failure
RS1-A	3	128.37	35.8	Ductile flexural failure
RS3-A		70.07	39.5	Ductile flexural failure
HS4-A		130.43	29.37	Combined flexural-shear failure with (considerable deformation)
HS6-A		139.37	40.0	Ductile flexural failure
HS8-A		131.63	41.1	Ductile flexural failure
HS10-A		137.90	35.387	Ductile flexural failure
HS11-A		127.93	37.7	Ductile flexural failure

effective depth (d) which decrease the flexural capacity of the slab. On the other hand, a reduction in overall depth will cause decreasing in stiffness and therefore larger deflection is expected.
Under load case (B), the results of R_u parameter ranging from (1.12 to 0.94) are given in Table 8. The load carrying capacity of slab HS5-B (R_w=23%) is higher than that in RS2-B by 11.6%. This increase refers to the action of the shear reinforcement along the shear span region and the reinforcement mesh at the slab flange. Even for slab HS7-B which has R_w equal to 29% the load capacity remains higher than the solid slab RS2-B by 5.7%. The comparison between HS5-B and HS7-B which produced an increase in R_w from (23 to 29%) and have the same details of the reinforcement with different ribs width is made. The load capacity of slab HS5-B is higher than slab HS7-B. The reason for that refers to the cracks development at the tensile zone. The development of cracks in the slab HS5-B is slower than in the slab HS7-B and this is due to the increase in the area of concrete which provides resistance to normal tensile stresses.

The results of slab HS9-B shows a reduction in the ultimate load capacity compared to the solid slab RS2-B by 6.4%. This specimen is provided by solid portion at each end and upper reinforcement mesh at slab flange. It was observed that there is no symmetry in crushing line on the upper face of specimen about x-axis as shown in Fig. 13. This indicates that the loads were not distributed on the ribs uniformly and at the same time. Therefore, the loads are concentrated on specific ribs and the failure occurs at load level lesser than the expected.

2.5.4 Modes of failure for tested slab specimens

In this section, the modes of failure with necessary data defined earlier are listed in Tables 9 and 10 under load cases (A) and (B) respectively.

Table 10 Failure mode for specimens tested under loading case (B)

Specimens	a/d	Ultimate load P_u (KN)	Displacement Δ_u at P_u (mm)	Mode of failure
RS2-B	2	215.80	40.2	Diagonal tension failure
HS5-B		240.76	40.6	Ductile flexural failure
HS7-B		227.90	40.0	Ductile flexural failure
H9-B		202.06	48.0	Diagonal tension failure

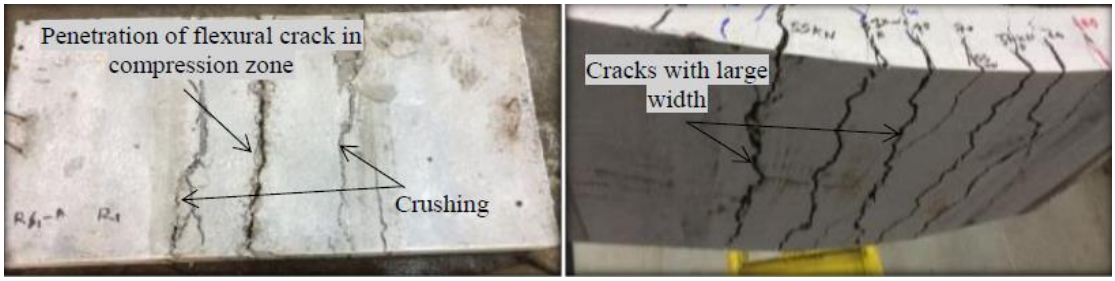

Fig. 14 Mode failure in slab RS1-A

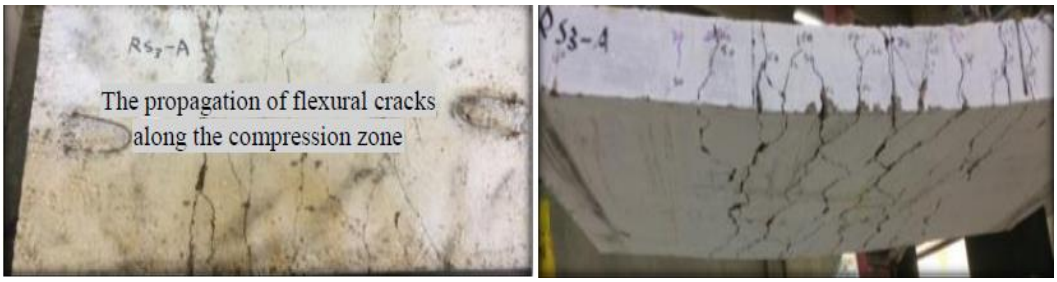

Fig. 15 Mode failure in slab RS3-A

It can be observed that all tested slab specimens failed after the tensile reinforcement reaches yielding with considerable deformation. On the other hand, the flexural cracks were formed at the slab bottom face, near the mid-span (within the pure bending region) and propagate upwards. Also, serious of cracks was formed at the shear span region. In contrast to the developed cracks in the solid slab which extend through the compression zone, the flexural cracks in the styropor block slab (along the pure bending region) vanish at upper reinforcement mesh location. The reinforcement mesh at flange contributed in resisting considerable tensile stress. The purpose of using shear reinforcement in slabs was to transform the failure mode from sudden behavior to ductile behavior and not to increase the slab load carrying capacity.

From Table 9, slab RS1-A is controlled by ductile flexural failure (under-reinforced). The failure occurred symmetrically by concrete crushing in two regions along the line of applied loads. The failure mode in the slab RS3-A is similar to slab RS1-A. Figs. 14 and 15 show the failure modes in both slabs RS1-A and RS3-A respectively.

HS4-A slab is controlled by the combined flexural-shear failure, as the concrete crushed at the compression zone (different locations along the width of slab). The flexural cracks along the shear span region rotate to form flexural-shear cracks with 45^o towards the loading point and finally the diagonal shear failure occurred at specific ribs. The shear failure was predicted theoretically as

Fig. 16 Mode of failure in slab HS4-A

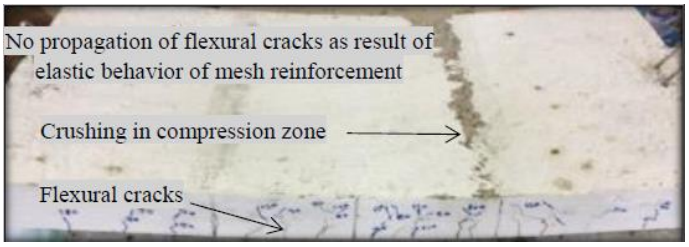

Fig. 17 Mode of failure in slab HS6-A

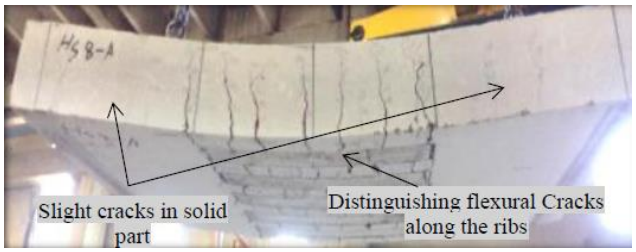

Fig. 18 Mode of failure in slab HS8-A

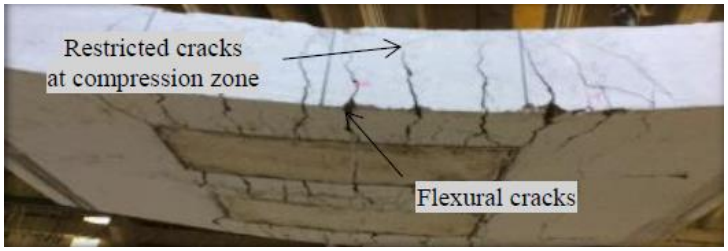

Fig. 19 Mode of failure in slab HS10-A

result of reducing the ribs width (b_w) in styropor block slab (HS) compared with overall width (B) in the solid slab (RS) which cause reduction in shear strength capacity (V_c). Fig. 16 shows the failure mode in slab HS4-A.

Slab HS6-A shown in the Fig. 17 is controlled by ductile flexural failure with largest ultimate load capacity under loading case (A). Strengthening the shear span region by shear reinforcement increase the shear strength capacity and improve the characteristic of concrete under the confinement state. HS6-A (weight reduction 29%) exhibits ductile behavior compared with slab HS4-A (weight reduction 23% and without shear reinforcement) under sudden behavior.

Fig. 20 Mode of failure in slab HS11-A

Fig. 21 Mode of failure in slab RS2-B

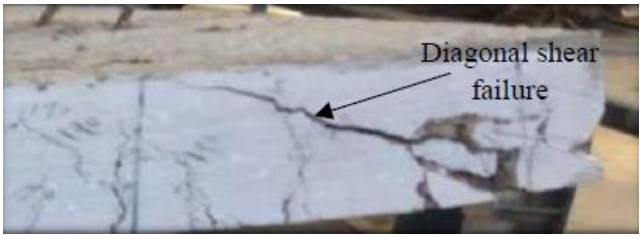

Fig. 22 Mode of failure in slab HS9-B

Fig. 23 Mode of failure in slab HS5-B

Figs. 18, 19 and 20 shows the failure modes in slabs HS8-A, HS10-A and HS11-A respectively. HS8-A and HS10-A slabs with solid portion at each end are controlled by ductile flexural failure. The failure modes were expected because a sufficient shear capacity (V_n=V_c) provided by solid slab portion which are similar to those in the solid slab RS1-A and also the loaded slab width (B) along the shear span is kept constant (compared to the slab HS4-A). HS11-A slab with variable cross-section along the shear span (a) is controlled by ductile flexural failure. HS11-A slab exhibits similar behavior compared to RS1-A, HS8-A and HS10-A.

Under load case (B), the slab RS2-B is controlled by diagonal tension failure. The slab HS9-B

Fig. 24 Mode of failure in slab HS7-B

with solid slab portion at the ends is failed in a similar manner to slab RS2-B. Figs. 21 and 22 show the mode failure of slabs RS2-B and HS9-B respectively.

The failure of HS5-B and HS7-B slabs which have weight reduction of 23% and 29% respectively and reinforced with shear reinforcement along a distance (0.3×effective span) are controlled by ductile flexural failure. HS5-B slab exhibits the largest value of ultimate load capacity under the load case (B), the comparison with the specimen HS7-B in this aspect may refer to the contribution of concrete under neutral axis which increased the load capacity. Figs. 23 and 24 show the mode failure of slabs HS5-B and HS7-B respectively.

Now, it can be concluded that all specimens are expected to fail in a brittle shear failure under the load case (B) if shear reinforcement are not used. Unlike the specimens under the load case (A) which have the ability to resist the shear stresses through the solid slab portion or even the variable cross- section that used at the expected critical shear zone.

3. Conclusions

The main conclusions drawn from this research are:

• Reduction in cross-sectional area of styropor block slab by 29% under the loading cases A and B with using minimum shear reinforcement exhibits an increase in strength capacity by 8.6% and 5.7% compared to the RS. This is observed in this study through the results of specimens HS6-A and HS7-B respectively.

• At the same level of reduction in cross-sectional area of styropor block slab and solid slab (specimens HS6-A and RS3-A) by 29% under loading case A, the styropor block slab strengthened by minimum shear reinforcement offers an increase in strength capacity by 98%.

• Despite the appearance of cracks in styropor block slabs with loads less than those in the reference slabs, the development of cracks in styropor block slabs during loading is slower than what observed in solid slab as results of presence the upper mesh reinforcement.

• The increase in cross sectional area of the ribs within the styropor block slab section shows improved results than the increase of the number of ribs at the same weight reduction percentage. Results of cracking load capacity were 63% and 77% of RS and of ultimate load capacity were 102% and 107% of RS for specimens HS8-A and HS10-A respectively.

• Alternative solutions to improve the shear strength capacity can be provided using solid slab portion or tapered cross section at critical shear region. The results of slab HS11-A with (R_w=29%) show strength capacity equaled to RS with similar failure mode.

• The best weight reduction percentages obtained in this study for styropor block slab ranging from (23% to 29%) with restricted condition of using minimum shear reinforcement along critical shear span region which provides sufficient strength capacity and suitable failure mode.

References

Abdul-Wahab, H.M. and Khalil, M.H. (2000), "Rigidity and strength of orthotropic reinforced concrete waffle slabs", *J. Struct. Eng.*, **126**(2), 219-227.

ACI 318 (2014), *Building Code Requirements for Structural Concrete and Commentary*, American Concrete Institute, Farmington Hills, Michigan, U.S.A.

Al-Azzawi, A.A. and Abed, S.A. (2017), " Investigation of the behavior of reinforced concrete hollow-core thick slabs", *Comput. Concrete*, **19**(5), 567-577.

Allawi, N.M. (2014), "Behavior and strength of one way voided reinforced concrete slabs", *Proceedings of the International Conference for Engineering Science*, University of AlMustansiriya, Baghdad, Iraq.

ASCE 7 (2005), *American Society of Civil Engineers: Minimum Design Loads for Buildings and Other Structures*, U.S.A.

Birgison, S.R. (2011), "Shear resistance of reinforced concrete beams without stirrup", B.Sc. Dissertation, Reykjav University, Iceland.

De Oliveira, D.R.C., Souza, W.M. and Caetano, T.R.G. (2014), "Shear strength of reinforced concrete one-way ribbed slabs", *RIEM-Revista IBRACON Estrut. Mater.*, **4**(5), 300-430.

EN 1992-1-1: Eurocode 2 (2004), *Design of Concrete Structures-Part 1-1: General Rules and Rules for Buildings*, European Committee for Standardization, Brussel, Belgium.

Gorkem, S.E. and Husem, M. (2013), "Load capacity of high-strength reinforced concrete slabs by yield line theory", *Comput. Concrete*, **12**(6), 819-829.

Lau, T.L. and Clark, L.A. (2011), "Shear design of wide beam ribbed slabs", *J. Inst. Eng. Malays.*, **72**(3), 231-239.

Olawale, A.J and Ayodele, A.G. (2014), "A comparative study on the flexural behavior of waffle and solid slab models when subjected to point load", *J. Civil Eng. Architect.*, **4**(5), 122-150.

Yu, L.D., Yang, Z. and Chai, X. (2016), "Test of concrete slabs reinforced with CFRP prestressed prism", *Comput. Concrete*, **18**(3), 355-366.

CC